

# Dynamic Contrast Enhanced MRI of Carotid Plaque: Comparison of Pharmacokinetic Models

M. E. Gaens<sup>1</sup>, S. Rozel<sup>1</sup>, M. Lipperts<sup>1,2</sup>, R. M. Kwee<sup>1</sup>, K. Jaspers<sup>1</sup>, M. J. Daemen<sup>1</sup>, J. E. Wildberger<sup>1</sup>, W. H. Backes<sup>1</sup>, and M. E. Kooi<sup>1</sup>

<sup>1</sup>Department of Radiology, Cardiovascular Research Institute Maastricht (CARIM), Maastricht University Medical Center, Maastricht, Netherlands, <sup>2</sup>Department of ICMT, Atrium Medical Center, Heerlen, Netherlands

## Objective

The rupture of an atherosclerotic plaque is a major cause of ischemic events, such as stroke and myocardial infarction. Plaque vulnerability has been linked to the formation of angiogenic microvessels within the plaque. It has been shown that dynamic-contrast enhanced MRI (DCE-MRI) allows the detection and quantification of this neovascularisation<sup>1</sup>. Pharmacokinetic models are used to describe and quantify the tissue enhancement in the plaque after injection of a contrast agent. However, the accuracy of the determined pharmacokinetic parameters is highly dependent on the chosen model. In the present study different models were evaluated with regard to their ability to describe DCE-MRI of carotid plaques.

## Materials and Methods

Three pharmacokinetic models (Patlak<sup>2</sup> (a), Extended Tofts<sup>3</sup> (b), Tofts<sup>3</sup> (c)) were compared in a group of 29 patients with moderate (50-69%) carotid stenosis. The differential equation of the two-compartment model and the three model solutions are given on the right.  $C$  is the concentration in plasma ( $p$ ) and total plaque ( $tot$ ),  $v$  is the fractional volume of plasma ( $p$ ) and extracellular extravascular space ( $e$ ).  $K^{trans}$  is the (transendothelial) volume transfer constant [ $\text{min}^{-1}$ ], which indicates both blood supply and permeability. Imaging was performed on a 1.5 T MRI scanner (Intera 1.5 T, Philips Healthcare, Eindhoven, The Netherlands) with a unilateral 47 mm diameter surface RF coil placed at the position of the carotid bifurcation. Dynamic images were acquired for 11 overcontiguous slices of 6 mm thickness, using a 3D spoiled gradient echo sequence with cardiac gating (TE=3ms, TR=12 ms,  $\alpha=35^\circ$ ,  $256^2$  matrix, FOV=100 x 100 mm<sup>2</sup>). Injection of the contrast agent (0.1 mmol/kg body weight of gadopentate dimeglumine) was started during the third dynamic scan using a power injector set to an injection rate of 0.5 ml/sec. Regions of interest (ROIs) in the plaque were drawn on a pre-contrast anatomic image and signal intensity curves were evaluated on a ROI-averaged basis. Analysis was performed using a standardized arterial input function (AIF) that was derived from three high temporal resolution scans and shifted to coincide with the injection of the contrast agent. Comparisons of the overall fit errors and the uncertainties for the pharmacokinetic parameters were performed to determine the best model. Furthermore, the effect of measurement time on the parameter estimation of the Patlak model was investigated using Monte Carlo simulations. For this, a model tissue residue function and the standard deviation of noise were determined from experimental datasets of 16 patients and the same AIF as in the analysis of the patient data was used.

$$\frac{dC_e(t)}{dt} = \frac{K^{trans}}{v_e} (C_p(t) - C_e(t))$$

$$C_{tot}(t) = v_p \cdot C_p(t) + K^{trans} \cdot \int_0^t C_p(\tau) \cdot d\tau \quad (a)$$

$$C_{tot}(t) = v_p \cdot C_p(t) + K^{trans} \cdot \int_0^t C_p(\tau) e^{-\frac{K^{trans}}{v_e}(\tau-t)} d\tau \quad (b)$$

$$C_{tot}(t) = K^{trans} \cdot \int_0^t C_p(\tau) e^{-\frac{K^{trans}}{v_e}(\tau-t)} d\tau \quad (c)$$

## Results

Typical enhancement curves for the three models are shown in Figure 1. Since the vascular term is neglected in the Tofts model, it cannot account for the first pass peak of the contrast agent. Consequently, the Tofts model had a significantly higher fit error than the other two models (Fig. 2).

Fit uncertainties for  $K^{trans}$  were  $20 \pm 2\%$ ,  $35 \pm 4\%$  and  $10 \pm 1\%$  (mean  $\pm$  SE) for Tofts, Extended Tofts and Patlak, respectively. For  $v_e$  the uncertainties were  $26 \pm 3\%$  and  $200 \pm 53\%$  for Tofts and Extended Tofts, respectively. Uncertainty in  $v_p$  was  $67 \pm 20\%$  for Extended Tofts and  $24 \pm 3\%$  for Patlak.

The simulation results (Fig. 3) show a decrease of the estimated  $K^{trans}$  values with measurement time for the Patlak model, thus indicating a bias in the estimation of  $K^{trans}$ .

## Discussion

Because of the relatively short measurement time little or no reflux can be seen in the signal intensity curves. Thus, an accurate estimation of  $v_e$  is not possible in the Tofts and Extended Tofts model. Because of parameter interaction this also affects the uncertainty in  $K^{trans}$ . Consequently, the  $K^{trans}$  uncertainty was lowest for the Patlak model, which does not include reflux. However, simulations show that a bias in the  $K^{trans}$  estimation of the Patlak model will occur for datasets in which reflux is present.

## Conclusion

The Patlak model appears to be most suited to describe DCE-MRI of atherosclerotic plaques with the currently used 8 minute protocol, since it shows the lowest fit error and uncertainty of the three models. For this feasibly long measurement time the inclusion of reflux in the kinetic modeling is not necessary and only leads to an increase of the uncertainties.

## References

1. Kerwin, WS et al., *Radiology* 2006, 241: 459-68;
2. Patlak C. et al., *J Cereb Blood Flow Metab* 1983, 3:1-7;
3. Tofts P. et al., *J Magn Reson Imaging* 1999, 10:223-232.

This research was supported by the Center for Translational Molecular Medicine and the Netherlands Heart Foundation (PARISK).

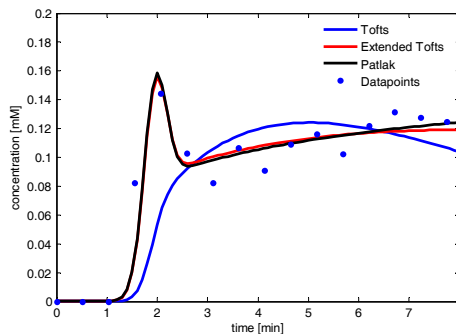


Figure 1: CA concentration in plaque as function of time and data fits using three different models

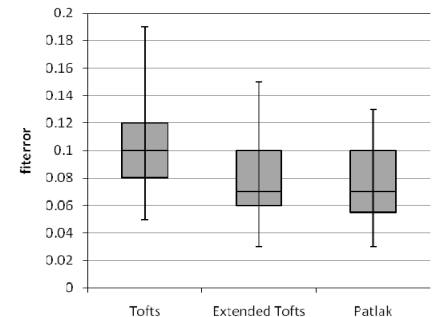


Figure 2: Fit error comparison for the three models. Shown are median (vertical line inside box), first and third quartile (boxes) and range (whiskers).

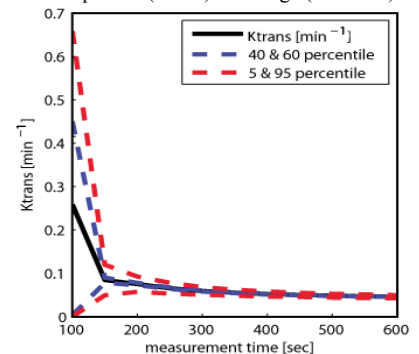


Figure 3: Simulation showing influence of measurement time on  $K^{trans}$  estimation for Patlak model (Monte Carlo randomization, 1000 runs).